J BONE ONCOL 40 (2023) 100483

Contents lists available at ScienceDirect

Journal of Bone Oncology

journal homepage: www.elsevier.com/locate/jbo

# Deep learning-based magnetic resonance imaging of the spine in the diagnosis and physiological evaluation of spinal metastases

Dapeng Wang [a,1], Yan Sun [b,1], Xing Tang [b], Caijun Liu [c], Ruiduan Liu [b,*]

[a] The Department of Traumatology, Affiliated Hospital of Guilin Medical University, Guilin 541001, China
[b] The Department of Spinal Surgery, Affiliated Hospital of Guilin Medical University, Guilin 541001, China
[c] The Third Affiliated Hospital of Guangzhou University of Chinese Medicine, Guangdong Research Institute for Orthopedics & Traumatology of Chinese Medicine, Guangdong 510378, China

## HIGHLIGHTS

- The research results show that the effective model method can effectively predict spinal metastasis with an accuracy of 96.45%.
- Softmax classifier is used to classify the results.
- The study of X-ray risk factors for fracture is of great significance.
- The depth model is realized to diagnose spinal MRI images, and finally the purpose of diagnosing spinal metastasis is achieved.
- The model obtained from the experiment can more accurately capture the focus signs of patients with spinal metastasis, and can predict the disease in time.

## ARTICLE INFO

*Keywords:*
Spinal metastases
Tumor
Magnetic resonance imaging
Physiological-based deep learning
Convolutional neural network

## ABSTRACT

*Background and objective:* Spinal metastasis accounts for 70% of the bone metastases of tumors, so how to diagnose and predict spinal metastasis in time through effective methods is very important for the physiological evaluation of the therapy of patients.
*Methods:* MRI scans of 941 patients with spinal metastases from the affiliated hospital of Guilin Medical University were collected, analyzed, and preprocessed, and the data were submitted to a deep learning model designed with our convolutional neural network. We also used the Softmax classifier to classify the results and compared them with the actual data to judge the accuracy of our model.
*Results:* Our research showed that the practical model method could effectively predict spinal metastases. The accuracy was up to 96.45%, which could be used to diagnose the physiological evaluation of spinal metastases.
*Conclusion:* The model obtained in the final experiment can capture the focal signs of patients with spinal metastases more accurately and can predict the disease in time, which has a good application prospect.

## 1. Introduction

Tumor is the leading cause of the high death rate in the world [1]. The most probable organ for tumors to metastasize is the liver, lungs, and bones [2]. Spinal metastases account for about 70% of bone metastases [3]. Pathological fractures occur in some patients with spinal metastasis, causing spinal nerve compression and nerve damage [4], seriously affecting the living quality and health, and consuming many medical resources and costs. Assessing the radiological risk factors for the progression of spinal metastasis to pathological compression fracture and predicting the prognosis of spinal metastasis can provide a more favorable basis for selecting interventional therapy by selecting a reasonable treatment mode before the patient's health deteriorates. The overall outcome of the physiological analysis of spinal metastases is deteriorating. Once a pathological compression fracture of the spine occurs, there is a risk of paralysis, which might result in a significant decline in the patient's health. Clinically, reasonable, adequate preventive treatment may prevent, reduce, or delay such adverse events if it is possible to predict which vertebral segments are about to suffer pathological fractures. The study of X-ray risk factors for fracture is of

* Corresponding author at: The Department of Spinal Surgery, Affiliated Hospital of Guilin Medical University, Guilin 541001, China.
*E-mail address:* spine@glmc.edu.cn (R. Liu).
[1] In this article, Dapeng Wang and Yan Sun make joint contributions.

https://doi.org/10.1016/j.jbo.2023.100483
Received 24 February 2023; Received in revised form 26 April 2023; Accepted 30 April 2023
Available online 9 May 2023

great significance.

The sensitivity and accuracy of MR in the physiological analysis of spinal metastases are significantly higher than that of X-ray and CT [5], which is determined by the physiological and pathological basis of the spine itself as well as various MR imaging methods. The typical vertebral body of the spine comprises three parts: bone tissue, cellular marrow, and fat marrow. The fat content of cellular marrow in the general adult vertebral body is 25 to 30 percent [6], with the gradual decrement of age, cellular marrow, and the gradual increases of fat marrow [7]. Fat marrow gets us a result with a significant signal on T1WI and a slight signal on T2WI compared to normal bone, providing a clear contrast. The metastasis and cellular marrow had affinity learning in predicting and diagnosing spinal metastases. Characteristics, so after tumor thrombus entered the vertebral body, metabolic changes were involved in the early period, and morphological and structural changes were formed later, resulting in pathological fracture [8]. After a tumor thrombus enters the vertebral body, the first damage is infiltrating the fat marrow in the blood vessel wall or the intercellular space extending along the blood vessel wall to form tumor tissue without destroying the morphological structure of the vertebral body [9]. Compared with vertebral fat marrow, the water content of tumor tissue is significantly increased, and the signal on T1WI is low, the signal on T2WI is high, and the STIR sequence is high, which is different from the mixed normal fat marrow in the vertebral body—signs of fat replacement. As the disease progresses, the vertebral structure is further damaged, and the compressed changes in the vertebral body gradually invade the surrounding soft tissue [9].

Our research aims to investigate the possibility of using deep learning to improve the diagnostic efficiency of spinal cord metastases in spinal MRI scans. Good spinal MRI scans will be used to train and test the deep learning model to determine the algorithm's feasibility.

## 2. Materials and methods

### 2.1. Data setting

This paper uses MRI scans of the spinal cord of tumor patients in the affiliated hospital of Guilin Medical University (see Fig. 1). After preliminary analysis, MRI scans of 305 patients with no signs of metastasis, 320 patients with mild signs of metastatic tumor, and 316 patients with apparent signs of metastatic tumor were finally classified. The data will be divided into a training set and a test set with a ratio of 8:2.

### 2.2. Preprocessing

For the collected data, format transformation should be carried out first. The magnetic resonance image format is unsuitable for deep learning model analysis. The Figuredata after format transformation should be processed in several ways, including filtering processing [10], denoising processing [11], segmentation processing, time correction processing, registration processing, resampling processing [12], smoothing processing, and other conventional preprocessing items. Finally, the processed magnetic resonance image is mapped to obtain the feature mapping map in the joint space.

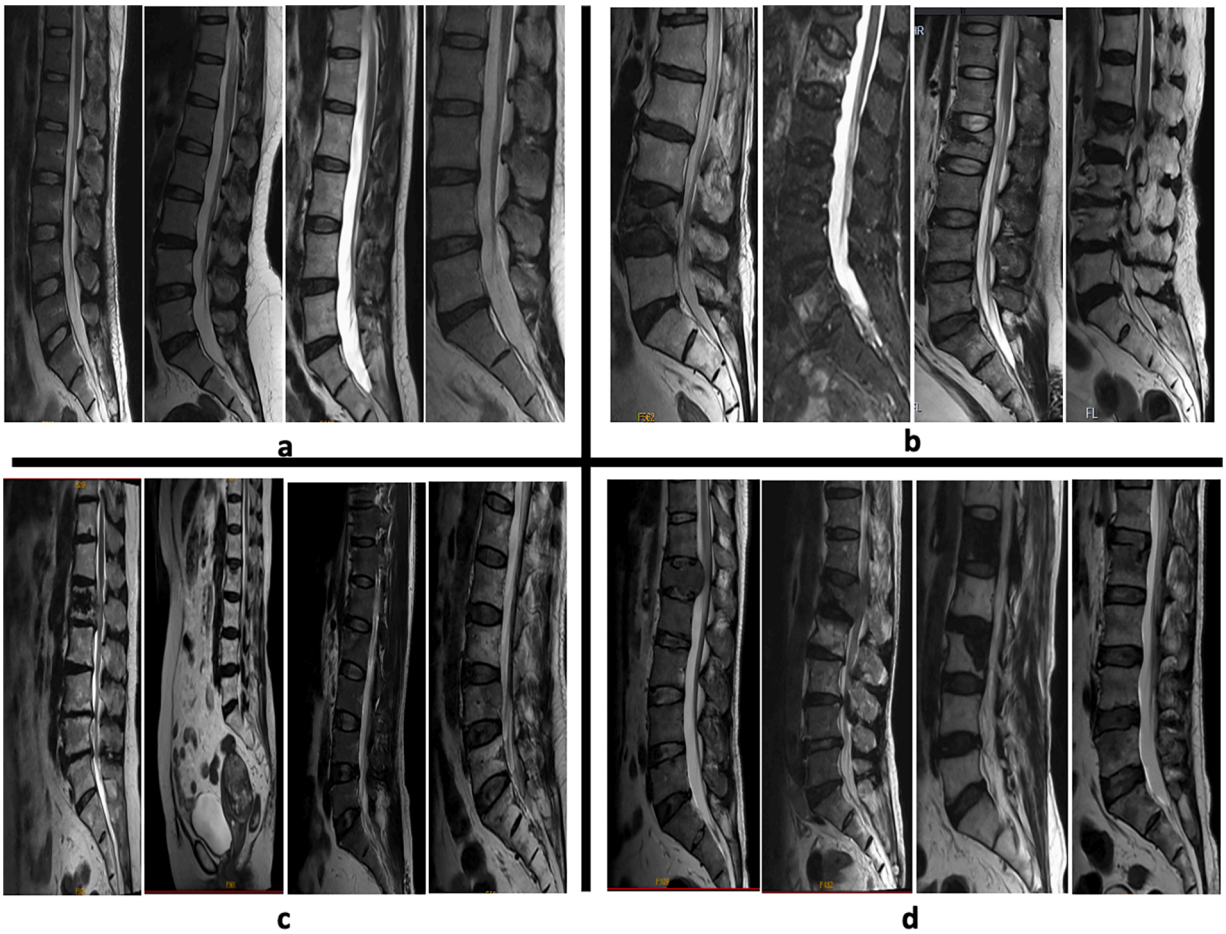


**Fig. 1.** Magnetic resonance imaging of the spine, (a) is a normal spine and (b) in patients with no signs of metastasis, (c) in patients with mild signs of metastasis, (d) in patients with apparent signs of metastasis. The red arrows point out the lesion. (For interpretation of the references to colour in this figure legend, the reader is referred to the web version of this article.)

### 2.3. Cognitive model construction

For spine MRI, the model we constructed is a multilayer convolutional neural network consisting of an input layer, together with multiple convolutional layers, at least one pooling layer, and at the same time, a fully connected layer. Considering the 3D nature of MRI, manifold learning is used to map 3D surfaces to 2D space. In this paper, we used the Gaussian geodesic process (GGP) method to define the relationship between the mapped and natural surfaces [13]. Convolutional Neural Network (CNN) will be what we mainly use to recognize distortion-invariant forms such as displacement and scaling of the two-dimensional diagram [14]. As the feature detection layer of the Convolutional Neural Network is learned from training data, explicit feature extraction would be expected to be avoided when using it, and implicit learning is used from training data instead [15]. At the same time, since neurons have the same weights in the feature map plane, the Neural Network can be concurrent learning, which shows the advantage of convolutional networks over neuron-connected networks [16]. The neural network has unique advantages in voice recognition [17] and image processing because of its unique local weight-sharing structure [18]. Its layout is closer to the actual biological neural network [19]. The weight sharing reduces the complexity network, especially since the multi-dimensional input vector can directly enter the network function to avoid the complexity and classification of data reconstruction in the function extraction function. The pooling layer is placed between the input layer and the complete connection layer, and the number of convolution layers is greater than the pooling layer.

The capacity of convolutional layers and pooling layers of the multilayer convolutional neural network can be appropriately increased or decreased according to the actual situation. When the sample capacity is large, the capacity of convolutional and pooling layers can be appropriately increased. Conversely, if the capacity of training samples is small, the capacity of convolutional and pooling layers can also be appropriately reduced.

Our three training filters and an additional bias convolution generated the image here. The filtering process is executed as described in Fig. 2. After the convolution, we obtain three feature maps generated in the C1 layer. Moreover, the three feature maps in the S2 layer are obtained through the SIGMOID function. Filter these diagrams to obtain the C3 layer. The structure of this level has produced S4, as is S2. In the end, we let these pixel values grid and connected to vectors to input the traditional neural network to generate outputs.

Generally, the C layer is a feature extraction layer in this system. Each neuron input example will be connected to the local acceptance field to the upper layer to extract local characteristics. The location's relationship with other characteristics will be determined once the local characteristics are extracted. The S layer is a feature mapping layer. Each computing layer of the network consists of multiple feature diagrams, and each plane of all neurons on the plane has the same weight. The characteristic mapping structure uses the SIGMOID function that affects the function which affects the function as a convolutional network, which makes the characteristic mapping level unchanged. In addition, the sharing weight of the neurons on the surface reduces the number of free parameters in the network and the complexity of the network parameter selection. Each feature extraction layer (C layer) in a convolutional neural network is followed by a computation layer (S layer) for local averaging and quadratic extraction. This unique dual-feature extraction structure gives the network high distortion tolerance for input sample recognition.

### 2.4. Training model

In essence, the convolution network is a mapping between input and output. During training, it understands much information about the relationship between input and output messages. Finally, it leads to concentrated feature vectors [20], representing the sample's nature. At the same time, there is no need to input the accurate mathematical expression of the input message and the outputs message, and the network can map inputs and outputs after training. This process involves two periods [19].

The first period is the favorable transmission period [21], where the sample is drawn and concentrated from the sample. X input in the CNN

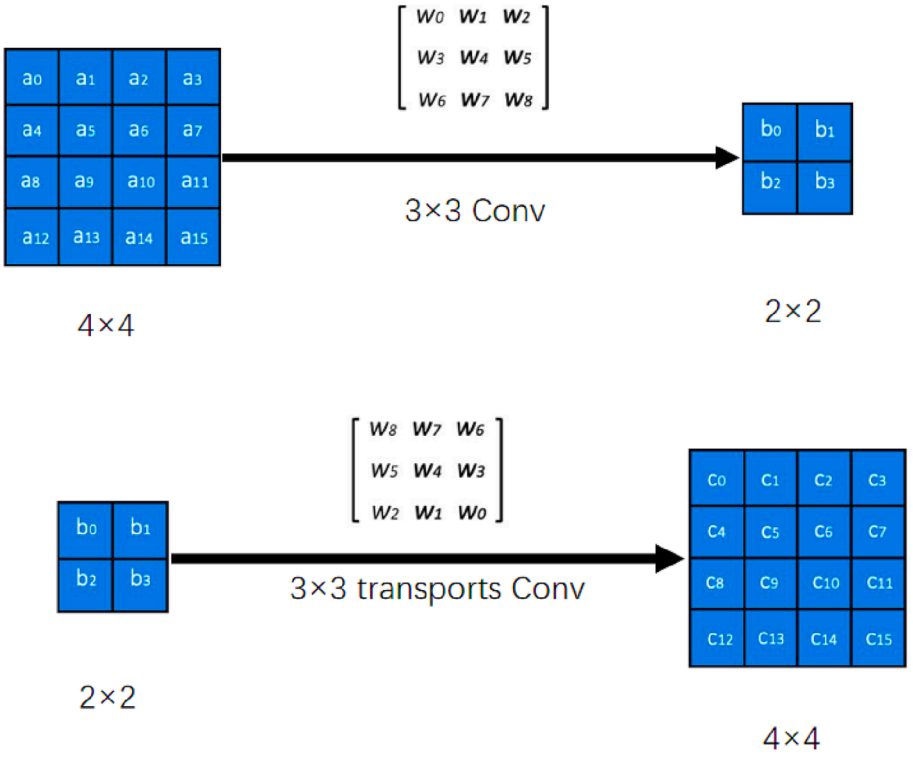


**Fig. 2.** Conceptual demonstration of CNN.

and the corresponding actual outputs is obtained after calculation (see Fig. 3). The information we need is transferred from the input layer to the outputs layer during this period. During this process, the network runs calculations. First, convolve to the convolutional layer; ap represents the outputs of the pooling layer, meaning there are s feature vectors, j represents the Jth row, and k represents the Kth column of its feature vector. w means the weight, I reveal the number of feature vectors of the next layer of neurons, s shows the number of feature vectors of the previous layer, m, and n shows us the value of the (m,n)th convolution kernel, b means bias, z is the input-sample of neurons in this layer, A is the outputs of neurons in this layer. Assume that both the horizontal and vertical steps of the convolution are d:

$$z_i^{l+1} = \sum_s a_s^l * w_{i,s}^{l+1} + b_i^{l+1} \tag{1}$$

$$a_i^{l+1} = sigmoid(z_i^{l+1}) \tag{2}$$

Then it continues to propagate forward from the convolutional layer to the pooling layer:

$$ap_i^l = pooling(a_i^l) \tag{3}$$

Finally, from pooling forward to the fully connected layer:

$$z_s^{l+1} = \sum_i ap_i^l w_{s,i}^{l+1} + b_s^{l+1} \tag{4}$$

The second period is the backward propagation period [22]. In the previous step, we obtained the actual outputs through calculation. The purpose of backpropagation is to achieve optimization and eliminate repetitive derivation steps.

$$\theta_{t+1} = \theta_t - \eta \frac{\partial(Loss)}{\partial \theta_t} \tag{5}$$

We will use this formula and chain rule backpropagation to achieve parameter update calculation.

### 2.5. Softmax classification

In the first steps, we finally get a complete feature vector. Finally, we must use the feature vector to make the final judgment on the MRI scans. In this step, we use the Softmax function to analyze it and get the final classification, namely, no signs of transfer, slight transfer, and apparent transfer, as shown in Fig. 4.

## 3. Results and discussion

Tumor is still the leading cause of death in patients. After the onset of the tumor, it is easy to metastasize from the site of the disease to other sites, resulting in the production of tumors in multiple sites of patients, which leads to the deterioration of the disease. Among these, bone metastasis is a significant physiology of metastatic sites. Spinal metastasis accounts for 70% of bone metastasis, and spinal metastasis often leads to many complications, affects the patient's nerves, and causes significant damage to the patient's health, resulting in severe consequences. Therefore, this paper considers an attempt to improve the predictive ability of spinal metastases through a means to predict the disease status for patients in advance to develop appropriate treatment programs for patients further and reduce pain of patients. Considering the outstanding achievement of deep learning models in medical diagnosis in recent years, this paper attempts to use deep learning to predict spinal metastases effectively.

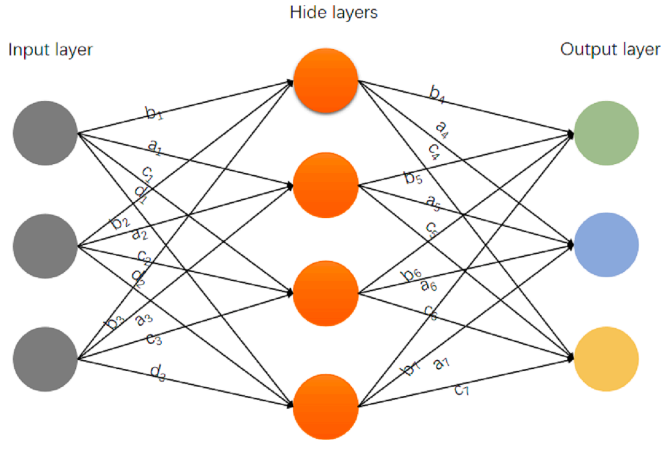


**Fig. 3.** Forward propagation of convolutional networks, the number above the line represents the weight value.

MRI is the most critical examination method for physiological analysis of spinal cord tumors; MRI plain scan and enhanced examination value is usually the highest. Tumors in the spinal cord usually show decreased signals in the central spinal cord on T1-weighted images, decreased signals at T1, and increased signals at T2. Astrocytoma has a fuzzy peripheral boundary with normal, whereas ependymoma has a relatively clear peripheral boundary with a regular spinal cord. Ependymoma is often accompanied by cystic change, fluid above and below, and central duct dilatation. On the enhanced scan, ependymoma, hemangioma, or reticulocyte of the spinal cord usually have marked enhancement. Astrocytomas, especially low-grade astrocytomas, have a low degree of enhancement, and high-grade astrocytomas have enhancement and uneven enhancement.

Hydrocephalic tumors must be distinguished from extra-spinal tumors, such as meningiomas, which usually intensify uniformly when enhanced and have a thickening of the adjacent meninges, known as the meningeal tail sign. The schwannoma intensifies and often grows outward along the foramina, forming a waxy or dumbbell shape. Extra-spinal bone metastases, and bone tumors, may present with the destruction of the spinal canal, vertebral body, or adnexa. Magnetic resonance examination is the first choice for spinal cord tumors. Based on the magnetic resonance findings, the surgical plan can be made to improve patients' curative effect and health of life. Therefore, this paper finally chooses deep learning to analyze MRI scans of the spinal cord and finally obtains the following results presented in Table 1.

We note that deep learning technology [23,24] can be applied to enhance medical care for diagnosis and physiological evaluation of spinal metastases related to the orthopedics field. Moreover, modeling bone cells coupled with understanding the cellular interactions [24] may have unpredictable high research value in tumor development and affecting cell structures, as well as spinal-related problems.

In this paper, we used deep learning to analyze and classify spinal magnetic resonance images to assist in the early diagnosis of spinal metastases. A multilayer convolutional neural network was trained to extract the features of MRI scans, and then the Softmax classifier was used to classify the extracted feature vectors. Three results were obtained: no signs of metastasis, slight and apparent signs of metastasis, and the highest accuracy was 96.45%, as shown in Table 1 and Fig. 5. The deep learning model significantly affects the prediction of spinal metastases in spinal MRI scans, which is essential for the early diagnosis of spinal metastases. It is worthy of further research and application.

## 4. Conclusion

In this paper, we implemented the depth model to diagnose spinal magnetic resonance images and finally achieved the purpose of diagnosing spinal metastases. A multilayer convolutional neural network was used for feature extraction of MRI scans to obtain feature vectors [25,26]. Meanwhile, Softmax was used to judge feature vectors to achieve the diagnosis effect. In conclusion, the model in this paper successfully and accurately diagnosed spinal metastases, and the accuracy of up to 96.54% can confirm that this model is worthy of being used in

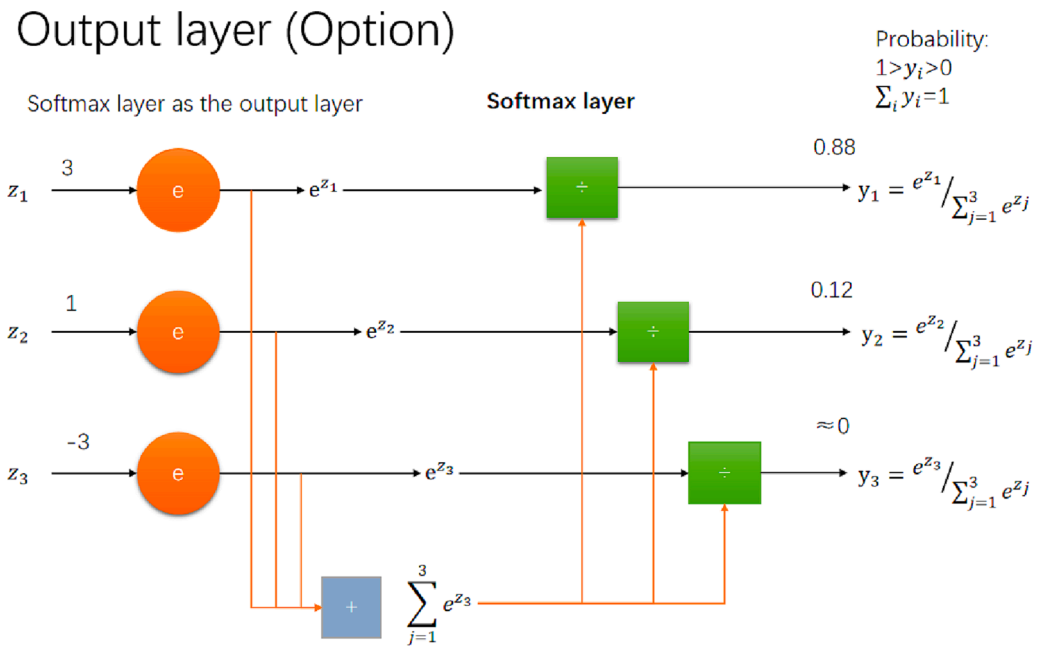


**Fig. 4.** Softmax outputs process.

**Table 1**
Using models to analyze the performance of each class.

| Class | accuracy | recall | F1 score |
|---|---|---|---|
| Class0 (Normal) | 0.9721 | 0.95 | 0.97 |
| Class1 (Mild metastases symptoms) | 0.9521 | 0.96 | 0.96 |
| Class2 (Significant metastases symptoms) | 0.9568 | 0.98 | 0.95 |

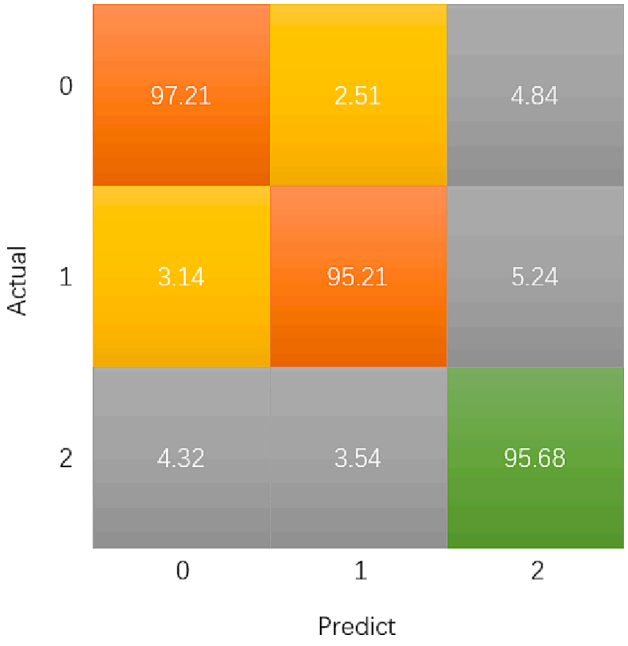


**Fig. 5.** Confusion matrix of the final model.

the early diagnosis of this disease.

**Ethical approval statement**

All the patients in this study have given written consent to the study.

**Fund statement**

This article is funded by the National Natural Science Foundation of China (82260442).

**Declaration of Competing Interest**

The authors declare that they have no known competing financial interests or personal relationships that could have appeared to influence the work reported in this paper.

**Data availability**

Due to certain privacy/moral restrictions, the author's request can provide data.

**References**

[1] N.G. Zaorsky, T.M. Churilla, B.L. Egleston, S.G. Fisher, J.A. Ridge, E.M. Horwitz, J. E. Meyer, Causes of death among cancer patients, Ann. Oncol. 28 (2) (2017) 400–407.
[2] V.R.D. Kakhki, K. Anvari, R. Sadeghi, A.-S. Mahmoudian, M. Torabian-Kakhki, Pattern and distribution of bone metastases in common malignant tumors, Nucl. Med. Rev 16 (2) (2013) 66–69.
[3] R.D. Rubens, Bone metastases—the clinical problem, Eur. J. Cancer 34 (2) (1998) 210–213.
[4] H.M. Barragán-Campos, J.-N. Vallée, D. Lo, E. Cormier, B. Jean, M. Rose, P. Astagneau, J. Chiras, Percutaneous vertebroplasty for spinal metastases: complications, Radiology 238 (1) (2006) 354–362.
[5] M.B. Lange, M.L. Nielsen, J.D. Andersen, H.J. Lilholt, M. Vyberg, L.J. Petersen, Diagnostic accuracy of imaging methods for the diagnosis of skeletal malignancies: A retrospective analysis against a pathology-proven reference, Eur. J. Radiol. 85 (1) (2016) 61–67.
[6] H. Kugel, C. Jung, O. Schulte, W. Heindel, Age-and sex-specific differences in the 1H-spectrum of vertebral bone marrow, J. Magn. Resonance Imag. 13 (2) (2001) 263–268.
[7] O. Gurevitch, S. Slavin, A.G. Feldman, Conversion of red bone marrow into yellow–cause and mechanisms, Med. Hypotheses 69 (3) (2007) 531–536.
[8] N. Jaffe, R. Spears, F. Eftekhari, R. Robertson, A. Cangir, Y. Takaue, H. Carrasco, S. Wallace, A. Ayala, K. Raymond, Y.-M. Wang, Pathologic fracture in osteosarcoma. Impact of chemotherapy on primary tumor and survival, Cancer 59 (4) (1987) 701–709.
[9] G. Maccauro, M.S. Spinelli, S. Mauro, C. Perisano, C. Graci, M.A. Rosa, Physiopathology of spine metastasis, Int. J. Surg. Oncol. 2011 (2011) 1–8.
[10] H. Moradmand, S.M.R. Aghamiri, R. Ghaderi, Impact of image preprocessing methods on reproducibility of radiomic features in multimodal magnetic resonance imaging in glioblastoma, J. Appl. Clin. Med. Phys. 21 (1) (2020) 179–190.
[11] J. Mohan, V. Krishnaveni, Y. Guo, A survey on the magnetic resonance image denoising methods, Biomed. Signal Process. Control 9 (2014) 56–69.

[12] J.J. Locascio, P.J. Jennings, C.I. Moore, S. Corkin, Time series analysis in the time domain and resampling methods for studies of functional magnetic resonance brain imaging, Hum. Brain Mapp. 5 (3) (1997) 168–193.
[13] C. Zhao, J. Lv, S. Du, Geometrical deviation modeling and monitoring of 3D surface based on multi-output Gaussian process, Measurement 199 (2022) 111569.
[14] X. Zhang, C. Xv, M. Shen, et al., Survey of convolutional neural network, in: 2018 International Conference on Network, Communication, Computer Engineering (NCCE 2018). Atlantis Press, 2018, pp. 93–97.
[15] A. Simkó, T. Löfstedt, A. Garpebring, et al., MRI bias field correction with an implicitly trained CNN, in: International Conference on Medical Imaging with Deep Learning. PMLR, 2022, pp. 1125–1138.
[16] A. Hernández-García, P. König, Further advantages of data augmentation on convolutional neural networks, in: Artificial Neural Networks and Machine Learning–ICANN 2018: 27th International Conference on Artificial Neural Networks, Rhodes, Greece, October 4-7, 2018, Proceedings, Part I 27. Springer International Publishing, 2018, pp. 95–103.
[17] O. Abdel-Hamid, L. Deng, D. Yu, Exploring convolutional neural network structures and optimization techniques for speech recognition, in: Interspeech. 2013, 2013, pp. 1173–1175.
[18] M.Z. Alom, M. Hasan, C. Yakopcic, et al., Recurrent residual convolutional neural network based on u-net (r2u-net) for medical image segmentation. arXiv preprint arXiv:1802.06955, 2018.
[19] T. Liu, S. Fang, Y. Zhao, et al., Implementation of training convolutional neural networks. arXiv preprint arXiv:1506.01195, 2015.
[20] A.A.A. Mohd Amiruddin, H. Zabiri, S.A.A. Taqvi, L.D. Tufa, Neural network applications in fault diagnosis and detection: an overview of implementations in engineering-related systems, Neural Comput. Appl. 32 (2) (2020) 447–472.
[21] W. Choi, K. Duraisamy, R.G. Kim, J.R. Doppa, P.P. Pande, D. Marculescu, R. Marculescu, On-chip communication network for efficient training of deep convolutional networks on heterogeneous manycore systems, IEEE Trans. Comput. 67 (5) (2018) 672–686.
[22] L. Shen, Z. Lin, Q. Huang, Relay backpropagation for effective learning of deep convolutional neural networks, in: Computer Vision–ECCV 2016: 14th European Conference, Amsterdam, The Netherlands, October 11–14, 2016, Proceedings, Part VII 14. Springer International Publishing, 2016, pp. 467–482.
[23] M. Zhao, Y. Wei, Y.u. Lu, K.K.L. Wong, A novel U-Net approach to segment the cardiac chamber in magnetic resonance images with ghost artifacts, Comput. Methods Programs Biomed. 196 (2020) 105623.
[24] X. Deng, Y. Zhu, S. Wang, Y.u. Zhang, H. Han, D. Zheng, Z. Ding, K.K.L. Wong, H. Zhang, CT and MRI determination of intermuscular space within lumbar paraspinal muscles at different intervertebral disc levels, PLoS one 10 (10) (2015) e0140315.
[25] Z. Zhang, J. Yang, A. Ho, W. Jiang, J. Logan, X. Wang, P.D. Brown, S.L. McGovern, N. Guha-Thakurta, S.D. Ferguson, X. Fave, L. Zhang, D. Mackin, L.E. Court, J. Li, A predictive model for distinguishing radiation necrosis from tumour progression after gamma knife radiosurgery based on radiomic features from MR images, Eur. Radiol. 28 (6) (2018) 2255–2263.
[26] B.o. Zhao, T. Cheng, X. Zhang, J. Wang, H. Zhu, R. Zhao, D. Li, Z. Zhang, G. Yu, CT synthesis from MR in the pelvic area using Residual Transformer Conditional GAN, Comput. Med. Imaging Graph. 103 (2023) 102150.